Measurements of the Low Frequency Gain Fluctuations of a 30 GHz High-Electron-Mobility-Transistor Cryogenic Amplifier

IN-33-CR
35201

Norman Jarosik

Abstract— Low frequency gain fluctuations of a 30 GHz cryogenic HEMT amplifier have been measured with the input of the amplifier connected to a 15 K load. Effects of fluctuations of other components of the test set-up were eliminated by use of a power-power correlation technique. Strong correlation between output power fluctuations of the amplifier and drain current fluctuations of the transistors comprising the amplifier are observed. The existence of these correlations introduces the possibility of regressing some of the excess noise from the HEMT amplifier's output using the measured drain currents.

Keywords— HEMT amplifiers, 1/f, radiometry, gain

1 INTRODUCTION

Recently major advances have been made in the noise performance and frequency range of ultra-low-noise cryogenic HEMT amplifiers [4]. One application which takes full advantage of both the low noise and large bandwidth of these amplifiers is radiometry in radio astronomy. High sensitivity in such radiometers is achieved both from the low noise temperatures and large instantaneous bandwidths of the amplifiers. The large bandwidths employed in turn require a very high degree of gain stability of the entire amplifier chain comprising the radiometer. After integrating for time τ the sensitivity achieved by a radiometer of bandwidth $\Delta\nu$ and noise temperature T is [3]

$$\delta T = T\sqrt{1/(\tau\Delta\nu) + (\delta g/g)^2} \tag{1}$$

where $\delta g/g$ is the mean magnitude of the fractional gain fluctuation occuring during the integration interval. As can be seen from the above relation, for a radiometer with $\Delta\nu = 3\,\mathrm{GHz}$ and $\tau = 1$ second, fractional gain fluctuations on the order of $\delta g/g \approx 10^{-5}$ will substantially degrade radiometer performance. In practice most radiometers employ some sort of Dicke switching [2] to circumvent such variabilities. Practical considerations limit the rate at which this switching can be performed making low frequency gain stability an important issue in radiometer design. This work attempts not only to characterize the low frequency gain stability of a cryogenic HEMT amplifier, but also to develop the techniques required to perform such measurements quickly and reliably, minimizing systematic errors introduced by the associated test equipment.

2 TECHNIQUE

The major obstacle in characterizing the stability of the HEMT amplifiers is that the other components used in performing the measurement typically have stabilities comparable to or worse than the HEMT amplifier under test. The resultant measurements therefore reflect not only the variability of the parameters of the amplifier under test, but also the variability of the components comprising the test setup.

The approach used here makes no assumptions about the stability or repeatability of the characteristics of most of the components of the test setup, rather it merely requires that the fluctuations inherent in two different sets of test components be uncorrelated. The technique is based on power-power correlations and is very similar to the operation of a Hanbury-Brown-Twiss radiometer [1]. A simplified description of this technique follows.

Assume that an amplifier under test is connected as shown in Fig. 1, with its input attached to a temperature stabilized load. Let the time dependent output power of the HEMT amplifier, $H(t)$, be given by

$$H(t) = \overline{H} + \delta H(t), \tag{2}$$

$$< \delta H(t) > \equiv 0, \tag{3}$$

where both the effects of noise temperature fluctuation and gain fluctuations of the HEMT amplifier are included in the term $\delta H(t)$, $\overline{H}$ denotes the mean value of the output power of the HEMT amplifier, and $<>$ denotes an average over a time long compared to the time scale of the fluctuations of interest. The output of the HEMT amplifier is then divided, amplified and detected by two (nominally) identical amplifier channels. The detected total power signals from the two outputs are described by

$$P_1(t) = H(t)G_1(t) = [\overline{H} + \delta H(t)]\,[(\overline{G_1} + \delta G_1(t)]\,, \tag{4}$$

$$P_2(t) = H(t)G_2(t) = [\overline{H} + \delta H(t)]\,[(\overline{G_2} + \delta G_2(t)]\,. \tag{5}$$

Here $\delta G_1(t)$ and $\delta G_2(t)$ represent the time varying components of the gains of room temperature amplifiers, and $\overline{G_1}$ and $\overline{G_2}$ are the mean gains of these amplifiers. (For simplicity the room temperature amplifier chains are assumed to have only gain fluctuations. This assumption is not neccesary, the only crucial assumption is that the time varying parameters of the two room temperature amplifier chains be uncorrelated.) In order to extract the HEMT characteristics the cross-correlation of $P_1(t)$ and $P_2(t)$ is formed:

$$\mathrm{Corr}(T) \equiv \int P_1(t)\cdot P_2(T-t)dt, \tag{6}$$

$$\begin{aligned}\mathrm{Corr}(T) = \int &[\overline{H} + \delta H(t)]\,[\overline{G} + \delta G_1(t)]\,\cdot \\ &[\overline{H} + \delta H(T-t)]\,[\overline{G} + \delta G_2(T-t)]\,dt.\end{aligned} \tag{7}$$

Princeton University, Department of Physics, Jadwin Hall, P.O. Box 708, Princeton, NJ 08544

Next, Corr(T) is ensemble averaged, recalling that the means of all the fluctuating components are defined as zero, and that all cross terms of δG_1, δG_2 and δH vanish as a result of their statistical independence. The only terms which survive the averaging are

$$< \mathrm{Corr}(T) >= \overline{H}^2\overline{G}^2 + \overline{G}^2 < \int [\delta H(T-t)\delta H(t)]dt >, \quad (8)$$

the second of which is proportional to the auto-correlation function of the fluctuating component of the power output of the HEMT amplifier which can be converted to a power spectrum by a Fourier transform. The effects of the variability of the parameters of the room temperature components are eliminated to the degree to which they are uncorrelated; the variability is manifest as additional statistical noise on the measured correlation functions and power spectra. Obtaining power spectra in this manner only picks out components which are correlated in the two data streams and can therefore be used to search for correlations between any time varying parameters in the radiometer.

Fig. 1 Simplified model of the radiometer used to explain the correlation technique.

3 APPARATUS AND DATA COLLECTION

The system used to make the measurements (Fig. 2) consists of both cryogenic and room temperature components [6]. The cryogenic components are two HEMT amplifiers, an orthomode coupler and a temperature regulated load. Each amplifer comes paired with a power supply which sets the operating point of each of the four transistors by fixing drain voltages and servoing the gate voltage to maintain a constant drain current. These amplifiers [5] have a gain of ≈30 dB from 25–35 GHz, and a mean noise temperature of ≈40 K when operated at a physical temperature of 15 K. The cryogenic components are located inside a vacuum-insulated dewar which is cooled by a mechanical refrigerator. The inputs of the two HEMT amplifiers are connected to the two single polarisation ports of the orthomode transducer, and the dual polarisation port is attached to a temperature regulated unpolarised load. The outputs of the two HEMT amplifiers are brought to a room temperature port on the dewar by two sections of stainless steel waveguide where they are connected to the room temperature amplifiers through isolators.

Fig. 2 Detailed block diagram of the radiometer employed in these measurements. The items enclosed in the dashed box were cooled to 15K by a closed cycle helium refigerator.

The room temperature components consists of two nominally identical channels, designated A and B. Each channel consists of a broadband amplifier and a frequency triplexer constructed from circulators and waveguide bandpass filters. The different frequency bands are designated 1, 2 and 3, and have nominal pass bands of 26–29, 29–32 and 32–35 GHz, respectively. A diode detector is located at the output of each band, and its output is fed into the data collection system where it is sampled at 64 Hz.

The data collection system has six channels designated A1, A2, A3, B1, B2, and B3, with the number corresponding to the frequency band and the letter indicating the radiometer channel.

4 MEASUREMENTS AND RESULTS

The room temperature amplifier chains were connected to the dewar output waveguides in different configurations, depending on the measurement being made.

4.1 Independent Channels

The first configuration employed was the same as shown in Fig. 2, in which the two radiometer channels are independent of one another apart from the orthomode coupler and the load. The spectral noise density measured at the output of all six detectors is very similar, Fig. 3 shows a representative spectrum obtained from the output of detector A1. The signals at the outputs of the detectors were processed as follows to produce spectra: first the time streams of data from the diode detectors representing the instantaneous output power of the radiometer were divided into blocks consisting of 1024 consecutive samples. After removal of the mean of each block, the block's auto-correlation function was formed. These auto-correlation functions were averaged, Fourier transformed and corrected for the frequency response of tha data collection system, yielding the power spectrum of the fluctuations of the output power of the radiometer. Each spectrum is normalised so that the mean value between 25 and 31.25 Hz (the Nyquist frequency) equals unity. This normalization compensates for the different losses, gains, and responsivities associated with the different channels and bands, and facilitates comparison of different spectra. The spectra from all six dectectors are similar and indicate an excess of noise at low frequencies, though from these data alone the source of this excess is not certain.

Fig. 3 Spectral density of the power fluctuations of the A1 channel of the radiometer obtained with the radiometer configured as in Fig. 2.

In this configuration, one expects the six radiometer outputs to be uncorrelated, aside from temperature fluctuations of the load. To test this prediction spectra are obtained by a procedure similar to that described above, except that rather than forming the auto-correlation of one of the detector outputs, a cross-correlation between two different outputs is employed. It should be noted that the power spectra calculated this way are not positive definite; in the situation where cross-correlations are formed, and the correlated signal in the two time streams is small compared to the random noise, negative values can result. The square-root of the magnitude of the power spectral density (dimensions of $\mathrm{K}/\sqrt{\mathrm{Hz}}$) is plotted on the ordinate in the following figures, and is displayed as negative if the value of the calculated power spectrum is negative. The normalisation for these cross-correlations is determined by using the appropriate combination of normalization constants derived from the auto-correlation of the two individual channels involved. For all combinations which correlate one output from the 'A' radiometer channel and one from the 'B' channel no significant correlations are observed, apart from a slight upturn at very low frequency. The solid line in Fig. 4 displays one of these spectra, obtained from the cross-correlation of outputs A1 and B1, typical of all nine 'AxB' cross-correlations. These spectra set a limit on the temperature stability of the load. Had there been significant temperature fluctuations of the load they would have been correlated for all combinations of outputs.

The dashed line in Fig. 4 shows a cross-correlation between frequency bands 1 and 2 within the 'A' radiometer channel. Here very significant correlations are evident. Similar spectra are obtained when cross-correlating any combination of frequency bands within either radiometer channel. The fact that all these spectra have similar shape and amplitude indicates that the output power of each radiometer channel is varying as a whole (i.e., equally and coherently across the entire RF bandwidth of the amplifier). Since the previous measurements precluded the possibility of variations in the emission from the load at this level, these fluctuations must be inherent in the radiometer itself.

Fig. 4 Spectral density of the power fluctuations obtained from the cross-correlations A1xA2 (dashed) and A1xB1 (solid) with the radiometer configured as in Fig. 2.

4.2 HEMT Amplifier Measurements

In order to directly observe the stability of a HEMT amplifier, the radiometer was reconfigured as shown in Fig. 5, where the output power from the HEMT is divided and then amplified by the two separate channels. The power spectra of the individual detector outputs are nearly identical, and are typified by the spectrum presented in Fig. 3, which was obtained with the radiometer in the original (indepedent channel) configuration. Fig. 6 shows the cross-correlations between channels 'A' and 'B', for combinations A1xB1, A2xB2 and A3xB3. These spectra represent the output power of the HEMT amplifier, with very little contamination from any of the other radiometer components. Since all these plots are time-averaged cross-correlations between the different room temperature channels, the effects of instabilities in the room temperature components are averaged out. All six cross-correlations between different channels and different frequency bands are very similar, representative combinations A2xB1 and A3xB2 are shown in figure 7. The fact that these other combinations are correlated and have nearly identical amplitudes and shapes strongly suggests that whatever instabilities are causing these correlations occur uniformly across the entire RF bandwidth of the HEMT amplifier. (The fact that the spectra in Fig. 6 all approach 1 in the high frequency limit while those in Fig. 7 do not is a result of the inherent statistical fluctuations in the power emitted by the load [1] which are correlated only when the passbands of the radiometer channels overlap.)

Fig. 5 The radiometer as configured to measure the HEMT amplifier's characteristics.

Fig. 6 Spectral density of the power fluctuations obtained from the cross-correlations between the same frequency bands of the two radiometer channels, A1xB1, A2xB2 and A3xB3.

Fig. 7 Spectral density of the power fluctuations obtained from the cross-correlation between different frequency bands of the two radiometer channels, A3xB2 and A2xB1.

4.3 Gain-Drain Current Correlations

In the course of performing these measurements it was noted that low frequency (.05– 10Hz) noise was present in the drain current of the individual transistors comprising the HEMT amplifier when the gate voltage was held constant. (The NRAO supplied bias circuitry was replaced with fixed voltage sources for these measurements.) The spectra of this noise was found to be similar that of the output power of the radiometer. The circuitry used to bias the transistors was carefully checked, and the source of these fluctuations was identified as the individual HEMT's comprising the amplifier.

Having determined that these fluctuations originate as variability inherent in the cyogenic transistors the question arises as to whether the fluctuations are related to fluctuations in the amplifier's output power. In order to determine this, four of the data collection channels previously connected to detectors A2, B2, A3, and B3 were used to monitor the drain currents of the four transistors in the HEMT amplifier. Fig. 8 shows the spectrum of fluctuations of the drain current of the input stage of the HEMT amplifier, again normalized to unity between 25 and 31.25 Hz. The spectra of the drain current fluctuations of the other transistors are similar in both character and magnitude. Cross correlations between the drain current time streams showed that there were no correlations between the drain current fluctuations of different transistors comprising the amplifier, consistent with the identification of the source of these fluctuations as arising from within the individual transistors.

To test for correlations between these fluctuations and the output power of the HEMT, cross-correlations between these drain currents and the detected power were obtained. Two representative spectra are presented in Fig. 9. Very significant correlations between the drain currents of each transistor and the detected output power are observed the magnitude of the correlation coefficient is ≈.2 dB/mA. and it has the sense that the gain increases as the drain currents increase. The fact that the magnitude of the correlations is roughly constant for the four different transistors, and that the fluctuations of the drain current are uncorrelated from transistor to transistor, indicates that *the observed drain current fluctuations are correlated to gain changes rather than noise temperature changes.* Had they been correlated to noise temperature changes, one would expect the correlations to be smaller for the transistors later in the amplifier chain, since the noise added by each successive gain stage is a smaller fraction of the overall system noise temperature. Similar results were obtained using the NRAO supplied bias circuitry which maintains the drain current and voltage of the individual transistors constant by servoing the gate voltage. In this case correlations between the gate voltages of the transistors and radiometer output power were observed, but *no improvement in the stability of the HEMT amplifier was achieved* .

Fig. 8 Spectral density of the drain current fluctuations of the first stage of the HEMT amplifier obtained with the gate and drain voltages held constant.

Fig. 9 Cross-correlations between output power of radiometer channel A1 and the drain current of the input transistor of the HEMT amplifier (A1xId1) and the drain current of the final transistor of the HEMT amplifier (A1xId4).

These measurements were repeated with the physical temperature of the amplifier at 12, 15 and 20 K, with no effect on any of the observed spectra. It was noted, however, that the temperature of the body of the HEMT amplifier varied 70 mK p-p coherently with the cycling of the mechanical refrigerator. The frequency of this oscillation is very stable at 1.2 Hz. The fact that no strong 1.2 Hz line is observed in any of the obtained spectra indicates that the amplifier's parameters are nearly temperature independent. A final set of measurements were made with the LEDs (light emitting diodes which illuminate the transistors) switched off. These data are presented in Fig. 10. There is a small improvement in stability at frequencies below ≈ 10 Hz when the LEDs are switched off. This improvement occurred immediately after the LEDs were extinguished, and no further changes were observed during the subsequent 12 hours.

Fig. 10 Spectral density of power fluctuations as obtained from the cross-correlations A1xB1 with the light-emitting-diode which illuminates the HEMTs ON (upper) and OFF (lower).

5 SUMMARY AND CONCLUSIONS

Accurate measurements of the stability characteristics of a 25–35 GHz HEMT amplifier have been obtained and with the amplifier's input attached to a 15 K temperature-regulated load. Measurements of the stability of the emission from the load indicate that temperature fluctuations of the load have a negligible contribution to these spectra, and the use of the power-power correlation technique has effectively eliminated sensitivity to fluctuations in the room temperature components. It appears that much of the variability is characterized by the gain of the amplifier shifting uniformly across its entire RF bandwidth, these variations being accompanied by changes in the drain currents of the individual transistors comprising the amplifier. The fact that these correlations exist raises the possibility of using the measured drain currents to regress some of the variability out of the data stream. Preliminary results have shown that ≈ 30% of the excess low frequency fluctuations can be removed using this technique.

The author would like to thank numerous people for their contributions to this work. First and foremost Marian Pospieszalski and Mike Balister of the National Radio Astronomy Observatory for the generous loan of the HEMT amplifiers. The exceptional performance of these amplifiers is revolutionizing many areas of observational radio astronomy. Ed Wollack and Barth Netterfield constructed respectively the radiometer and data collection systems used in this work. Thanks are also extended to Lyman Page, David Wilkinson and Suzanne Staggs for many discussions and help in preparation of this manuscript. This work has been supported by JPL contract # 959556 and NSF grant NAGW-2801.

REFERENCES

[1] R.H. Brown and R.Q. Twiss *A New Type of Interferometer for Use in Radio Astronomy*, Phil. Mag., vol. 45 pp. 663-682., July, 1954

[2] R. H. Dicke *The Measurement of Thermal Radiation at Microwave Frequencies*, Rev. Sci. Instr., vol. 17, pp. 268-275, July, 1946

[3] J. D. Kraus *Radio Astronomy*, p 7-12, Cyngnus-Quasar Books, Powell OH.

[4] M. W. Pospieszalski *Cryogenically-Cooled, HFET Amplifiers and Receivers: State of the Art and Future Trends*, IEEE MTT-S Int. Microwave Symp., pp. 1369-1372 Albuquerque NM, June 1992.

[5] M. W. Pospieszalski, J. D. Gallego and W. J. Lakatosh *Broadband, Low-Noise, Cyrogenically-Coolable Amplifiers in 1 to 40 GHz Range*, in Proc. 1990 Int. Microwave Symp., pp 1253-1256, Dallas, TX, May 1990.

[6] E. J. Wollack Princeton University thesis (1994).

Norman C. Jarosik received both his B.S. and Ph.D. degrees in physics from SUNY at Buffalo concentrating on two-dimensional electronic systems. From 1987 to 1989 he held a Postdoctoral position at Bell Laboratories where he studied phonons in dimensionally confined systems. Since 1989 he has been with the Department of Physics at Princeton University making measurements of the Cosmic Microwave Background Radiation.

Fig. 1. Simplified model of the radiometer used to explain the correlation technique.

Fig. 2. Detailed block diagram of the radiometer employed in these measurements. The items enclosed in the dashed box were cooled to ~15K by a closed cycle helium refigerator.

Fig. 3. Spectral density of the power fluctuations of the A1 channel of the radiometer obtained with the radiometer configured as in Fig. 2.

Fig. 4. Spectral density of the power fluctuations obtained from the cross-correlations A1xA2 (dashed) and A1xB1 (solid) with the radiometer configured as in Fig. 2.

Fig. 5. The radiometer as configured to measure the HEMT amplifier's characteristics.

Fig. 6. Spectral density of the power fluctuations obtained from the cross-correlations between the same frequency bands of the two radiometer channels, A1xB1, A2xB2 and A3xB3.

Fig. 7. Spectral density of the power fluctuations obtained from the cross-correlation between different frequency bands of the two radiometer channels, A3xB2 and A2xB1.

Fig. 8. Spectral density of the drain current fluctuations of the first stage of the HEMT amplifier obtained with the gate and drain voltages held constant.

Fig. 9. Cross-correlations between the output power of radiometer channel A1 and the drain current of the input transistor of the HEMT amplifier (A1xId1) and the drain current of the final transistor of the HEMT amplifier (A1xId4).

Fig. 10. Spectral density of power fluctuations as obtained from the cross-correlations A1xB1 with the light-emitting-diode which illuminates the HEMTs ON (upper) and OFF (lower).

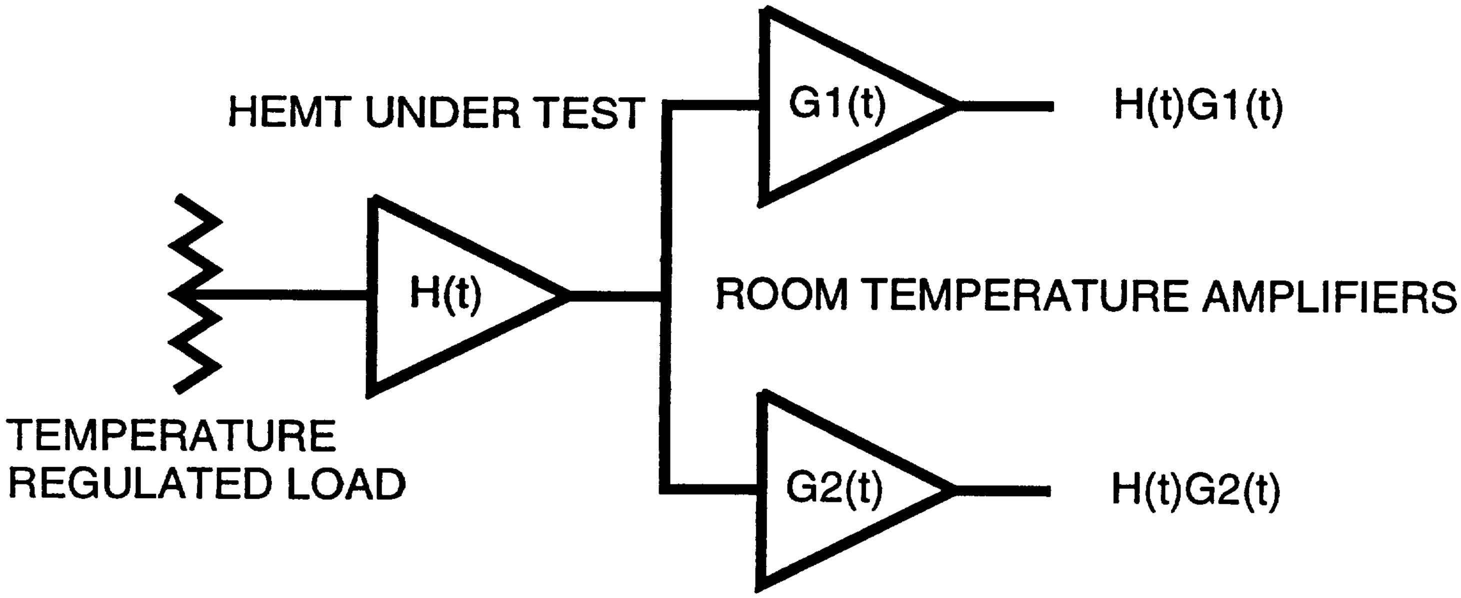
HEMT UNDER TEST
G1(t)
H(t)G1(t)
H(t)
ROOM TEMPERATURE AMPLIFIERS
TEMPERATURE
REGULATED LOAD
G2(t)
H(t)G2(t)

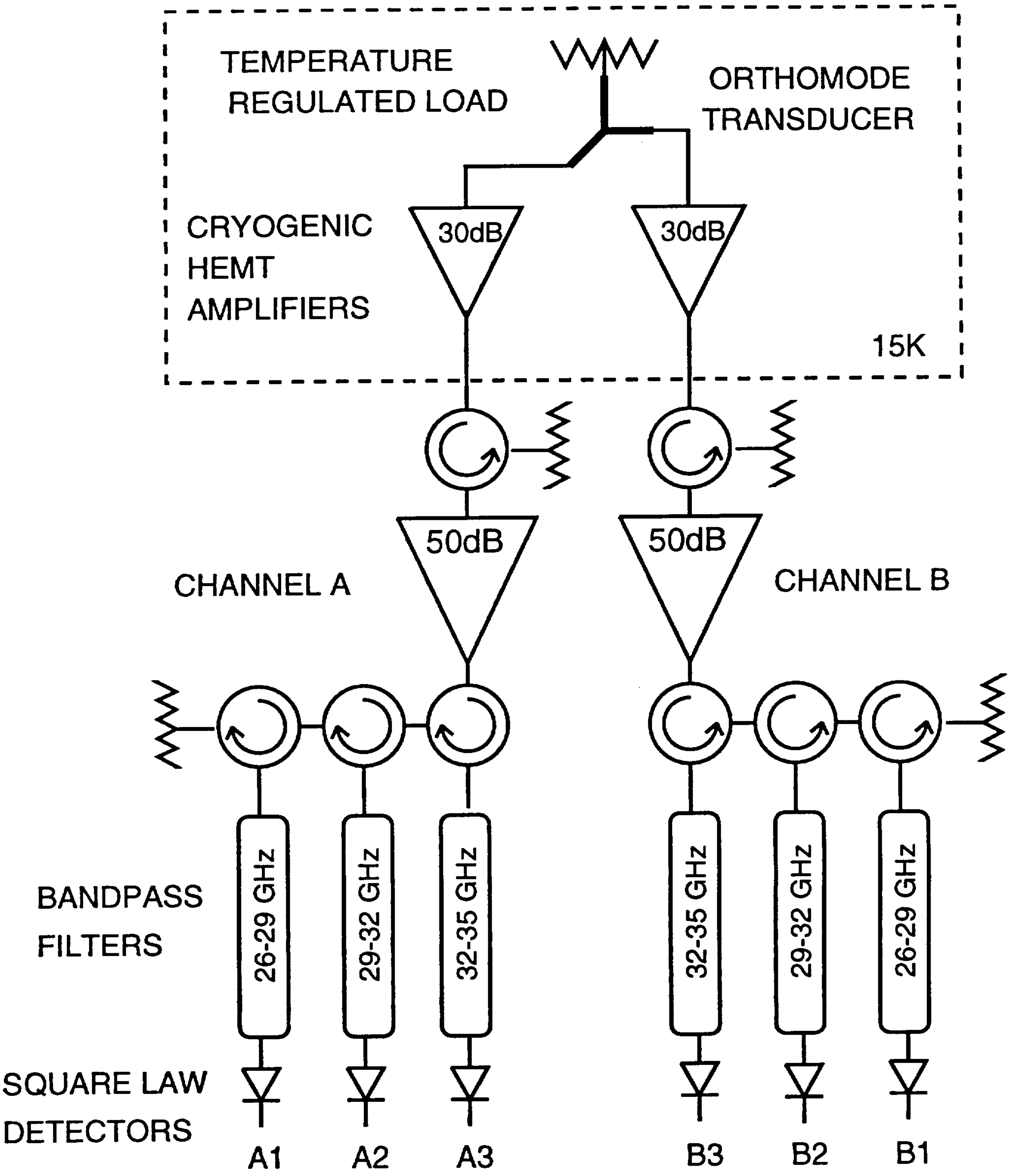
TEMPERATURE
REGULATED LOAD
ORTHOMODE
TRANSDUCER
CRYOGENIC
HEMT
AMPLIFIERS
30dB
30dB
15K
50dB
50dB
CHANNEL A
CHANNEL B
BANDPASS
FILTERS
26-29 GHz
29-32 GHz
32-35 GHz
32-35 GHz
29-32 GHz
26-29 GHz
SQUARE LAW
DETECTORS
A1
A2
A3
B3
B2
B1

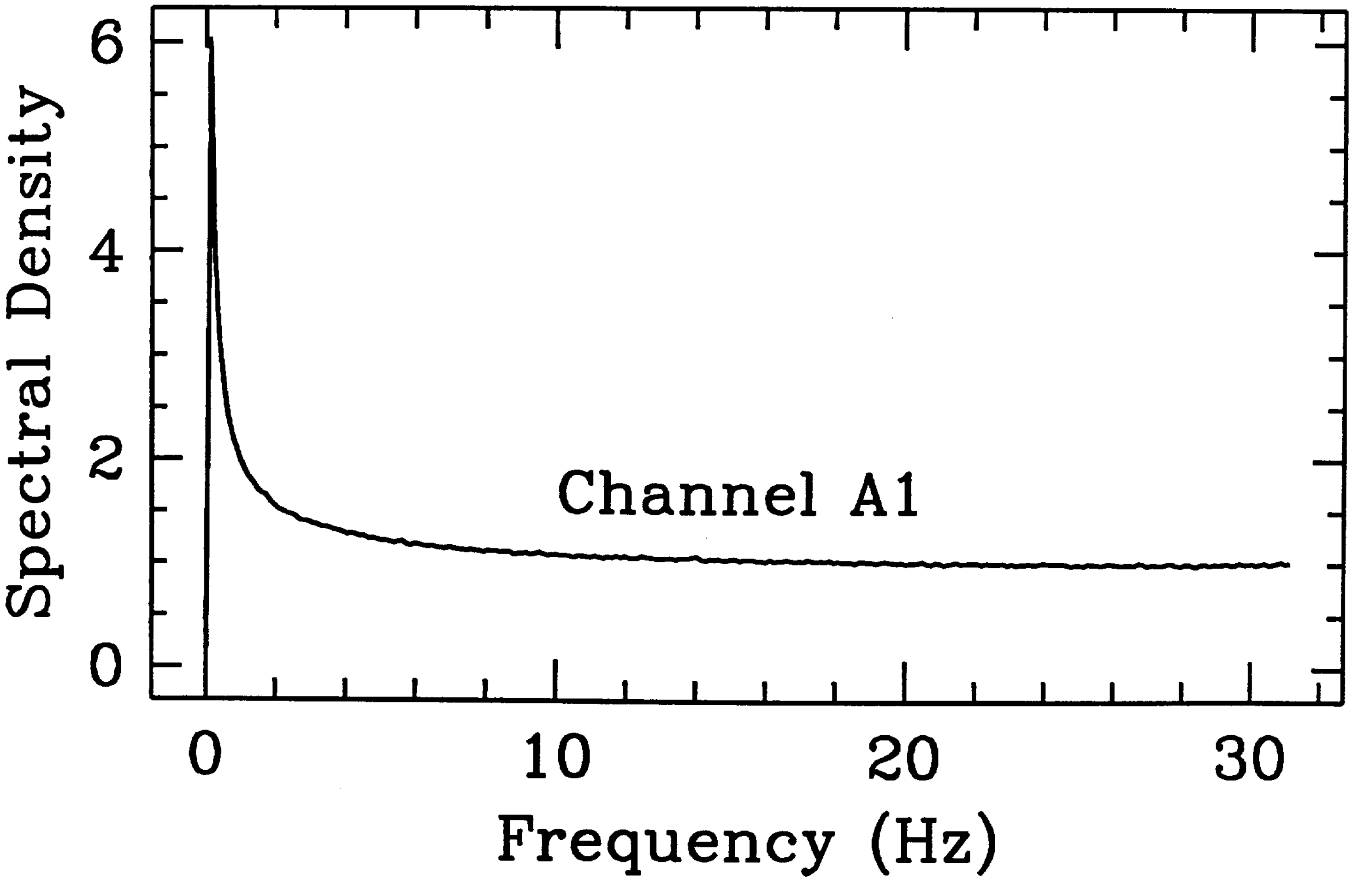
Spectral Density
6
4
2
0
0
10
20
30
Frequency (Hz)
Channel A1

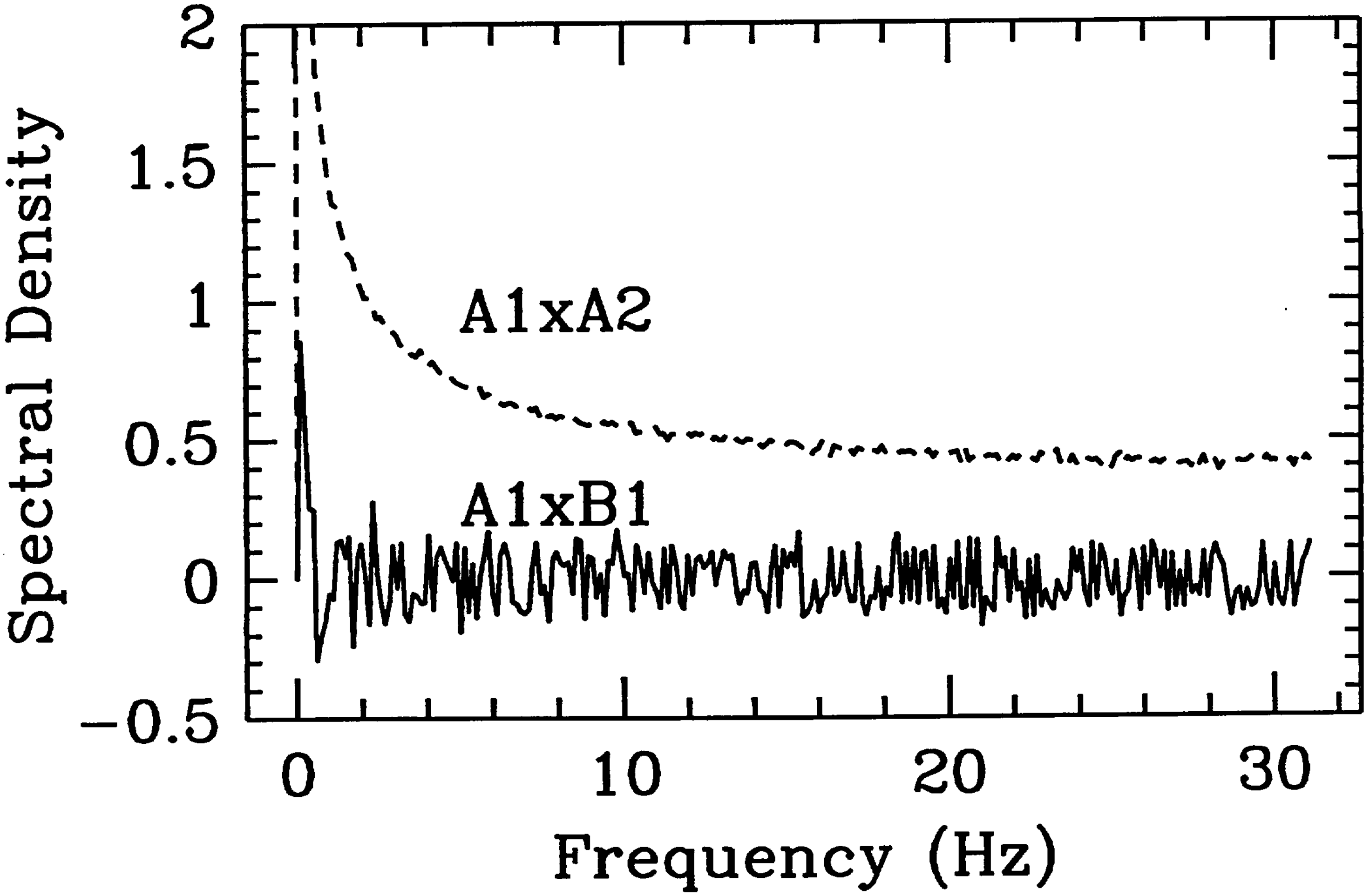
Spectral Density
2
1.5
1
0.5
0
−0.5
A1xA2
A1xB1
0
10
20
30
Frequency (Hz)

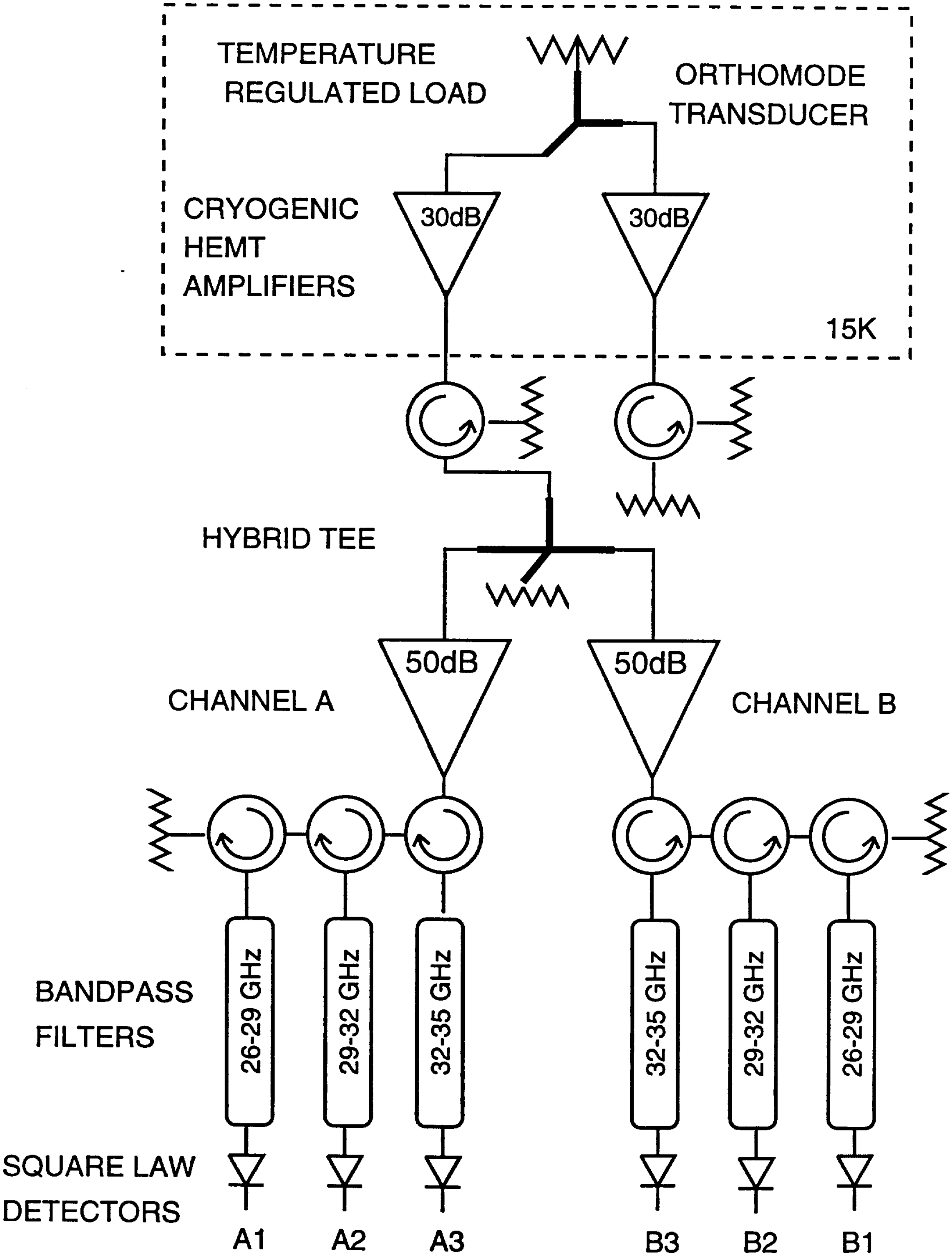
TEMPERATURE REGULATED LOAD
ORTHOMODE TRANSDUCER
CRYOGENIC HEMT AMPLIFIERS
30dB
30dB
15K
HYBRID TEE
50dB
50dB
CHANNEL A
CHANNEL B
BANDPASS FILTERS
26-29 GHz
29-32 GHz
32-35 GHz
32-35 GHz
29-32 GHz
26-29 GHz
SQUARE LAW DETECTORS
A1
A2
A3
B3
B2
B1

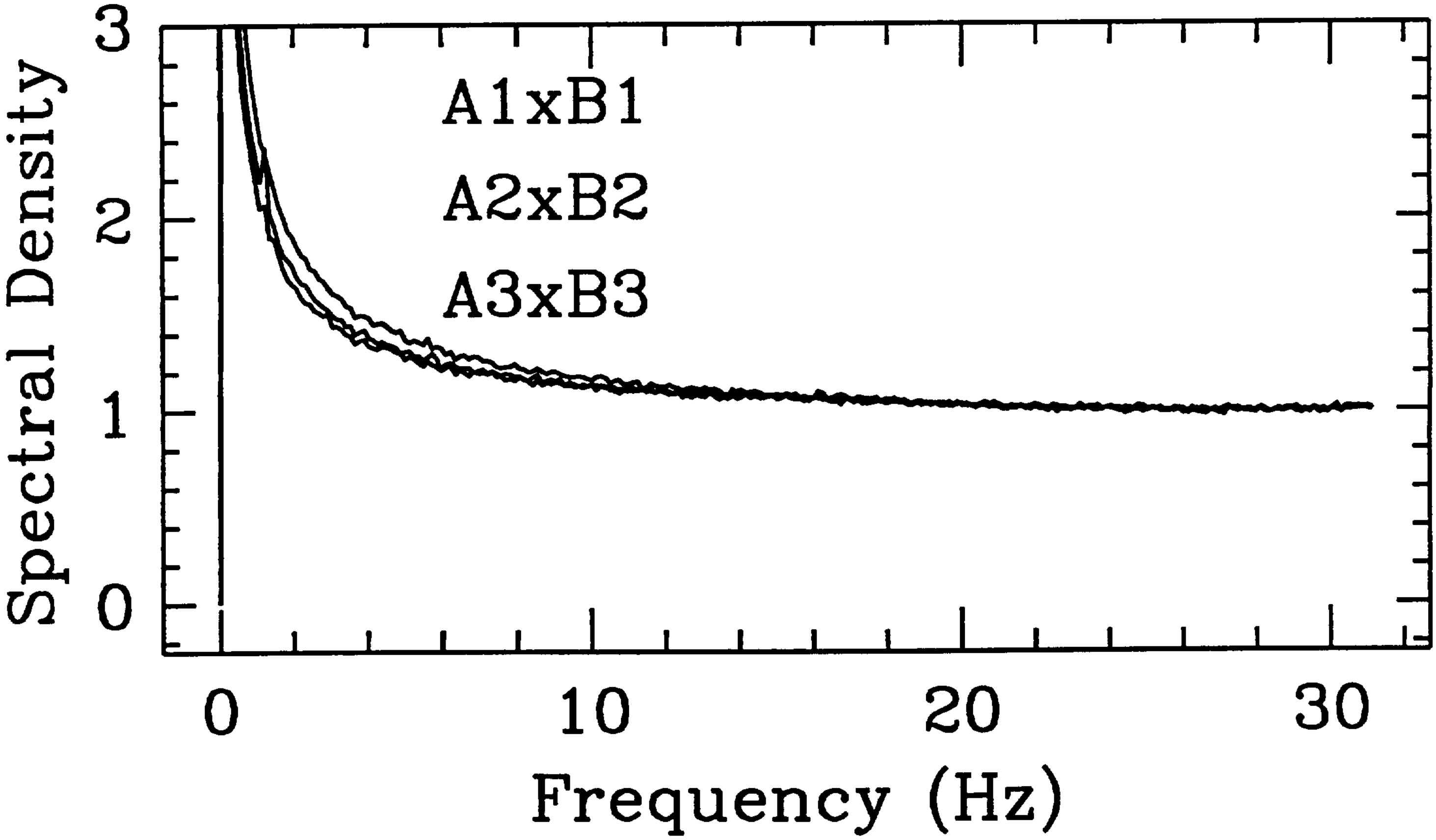
Spectral Density
3
2
1
0
A1xB1
A2xB2
A3xB3
0
10
20
30
Frequency (Hz)

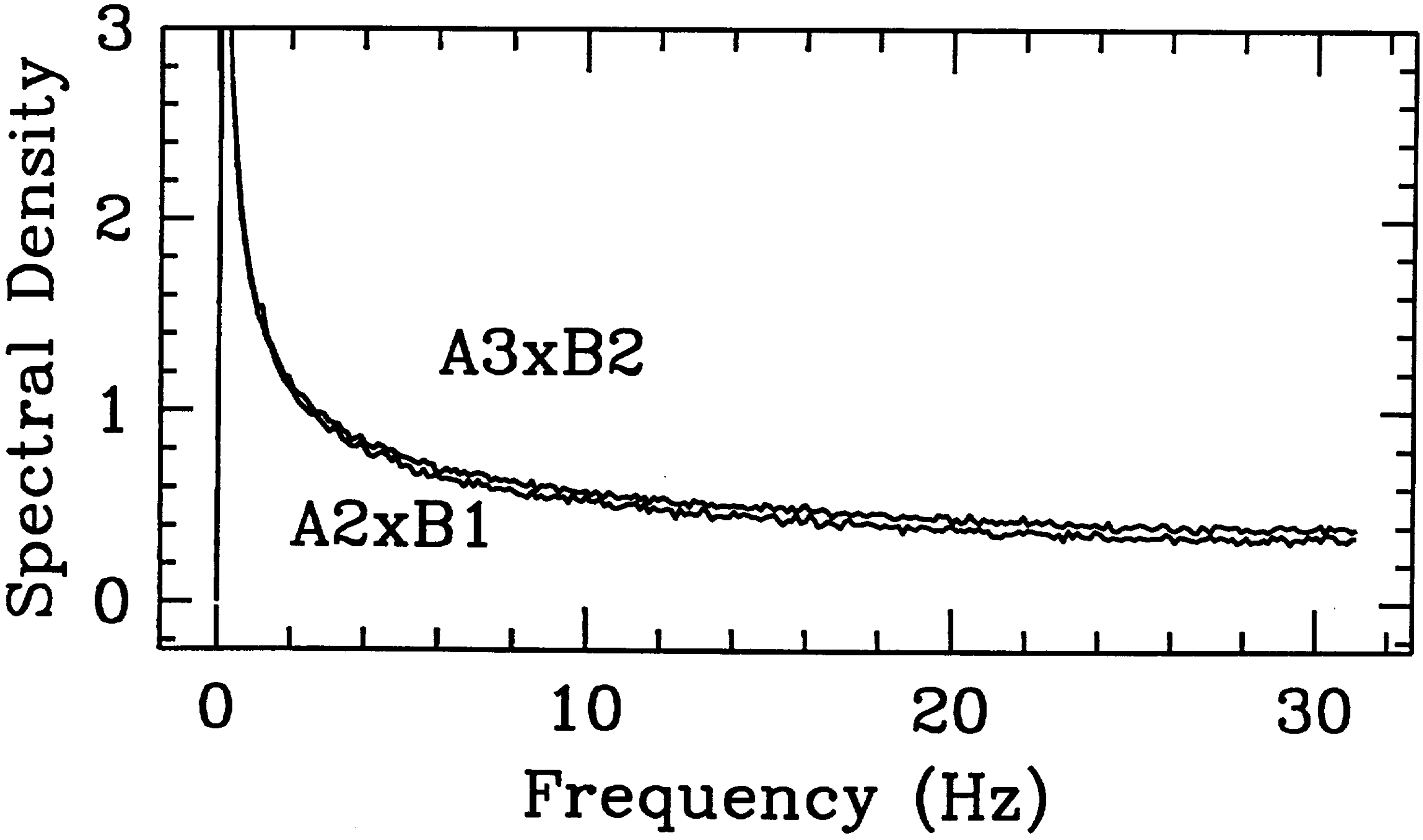
Spectral Density
3
2
1
0
A3xB2
A2xB1
0
10
20
30
Frequency (Hz)

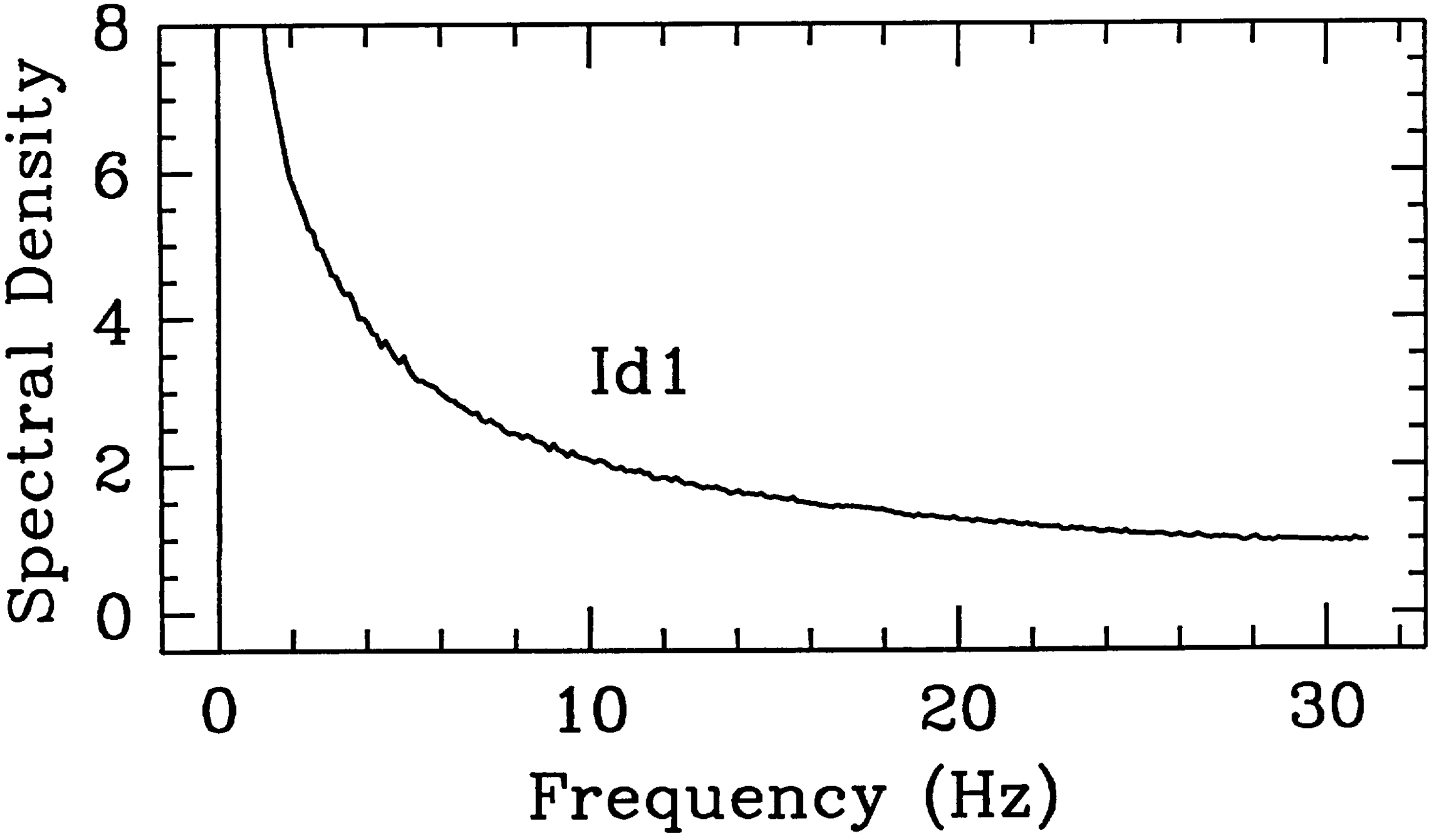
Spectral Density
0
2
4
6
8
0
10
20
30
Frequency (Hz)
Id1

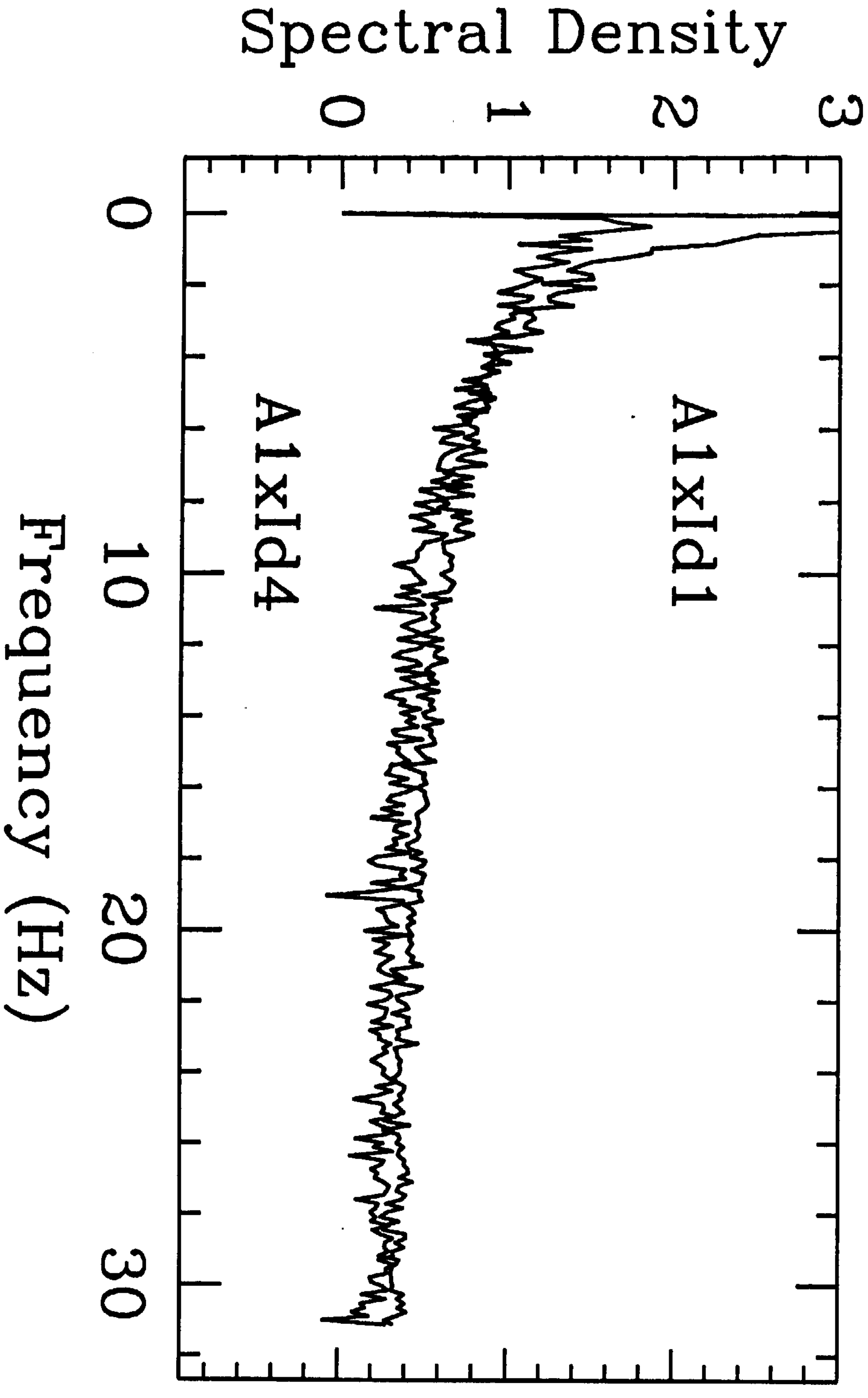
Spectral Density
0
1
2
3
0
10
20
30
Frequency (Hz)
A1xId1
A1xId4

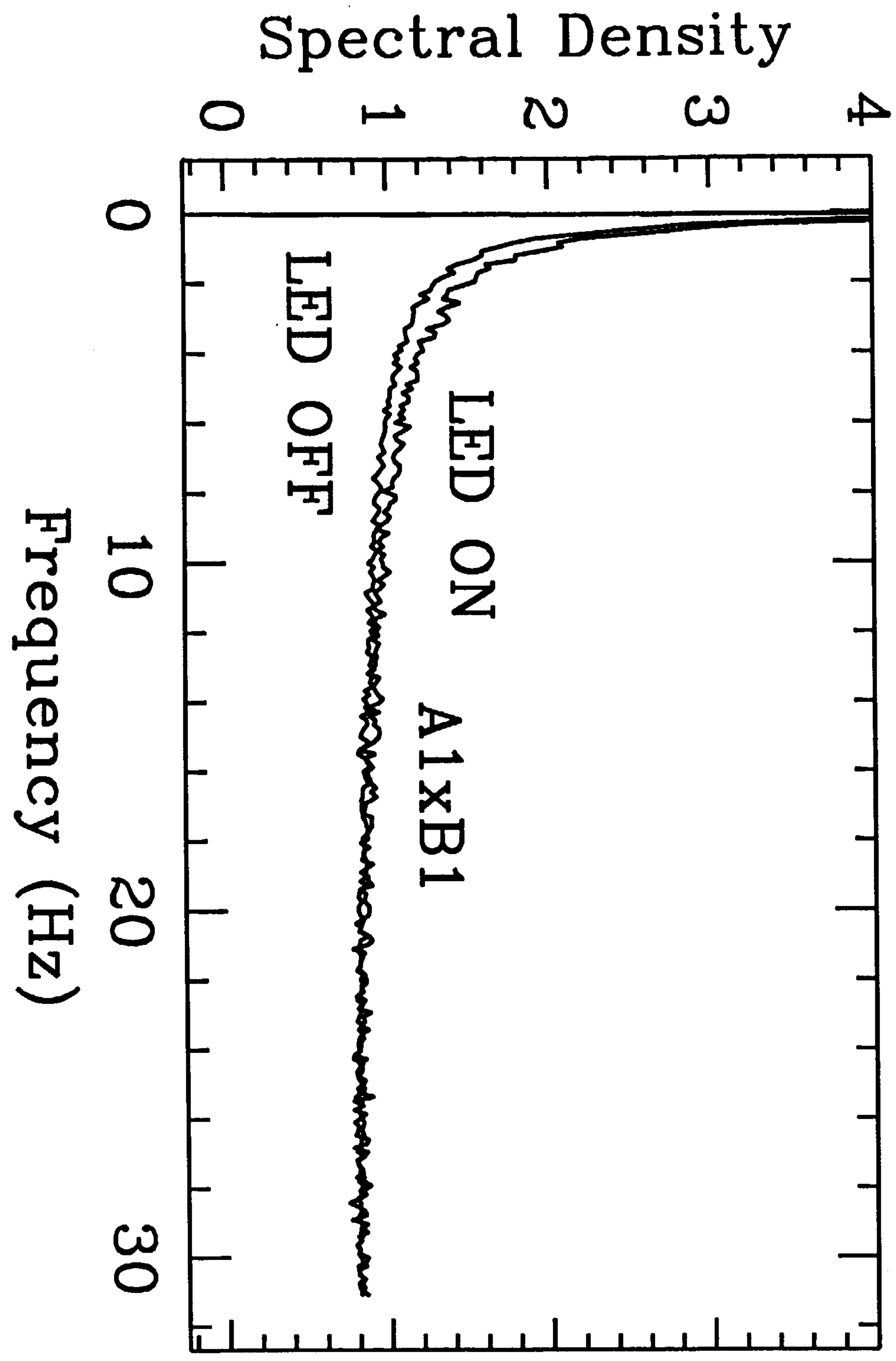
Spectral Density
0
1
2
3
4
0
10
20
30
Frequency (Hz)
LED ON
LED OFF
A1xB1